P-ISSN 2586-9000
E-ISSN 2586-9027
Homepage : *https://tci-thaijo.org/index.php/SciTechAsia* **Science & Technology Asia**
Vol. 27 No.4 October - December 2022 Page: [330-342]
Original research article

Using Disturbance Observer for Disturbance Rejection of DC Motor Trajectory Control Systems without Current Feedback

Pinit Ngamsom*

Department of Mechanical Engineering, Rangsit University, Pathum Thani 12000, Thailand

Received 8 February 2022; Received in revised form 8 June 2022;
Accepted 14 June 2022; Available online 31 December 2022

ABSTRACT

We employ the concept of disturbance observer to obtain an auxiliary linear controller that can be augmented to existing linear controllers for the primary purpose of disturbance rejection in DC motor trajectory control systems. Our development is all in state space and does not require feedback of current in motor coils. Uncertain time-varying parameters in the system matrix and the input matrix are allowed, and a simple sufficient condition for asserting robust input-to-state stability of the resulting control system is provided. It appears in numerical simulations that the proposed auxiliary control can reduce magnitude of tracking error and output oscillation due to persistent high-frequency disturbance by approximately 40%. Primarily, it achieves this by reacting quickly to changes in disturbance, not by increasing magnitude of the control signal. This allows its application in existing control systems without need to enlarge capacity of the associated amplifiers.

Keywords: DC motor; trajectory, disturbance; observer; stability

1. Introduction

Brush DC Motors have been actuators of choice in trajectory control systems because of their economical price, hardware simplicity, and strong torque delivery. Additionally, their simple dynamical characteristics facilitate design of drives and controllers. The armature of these motors could be skewed, and be designed to house sufficiently many lapping coils so that the resulting torque ripple due to mechanical commutation is insignificant. However, their principle of operation is associated with a few arch disadvantages. One of these is that the commutation employs mechanical brushes. These crucial parts wear out over

***Corresponding author:** ngamsomp@hotmail.com

time due to sliding contact they make with the commutator. This dictates that they are not suitable for high-speed applications in which periodical services are inconvenient. This disadvantage has been removed by introducing electronic commutation for brushless DC (BLDC) motors. A BLDC motor with trapezoidal back EMF usually has 3 phases. To gain simplicity and cost effectiveness, the motor is usually driven by using 6 steps of electronic commutation [1, 2] for which relevant hardware is generally enclosed separately from the motor. In each of these steps, 2 out of 3 sets of stator coils are to be driven sequentially by square-wave current. In practice, this yields a large torque ripple due to strong stepwise rotating magnetic field and nonideal current waveform [2-5]. The ripple occurs very rapidly in every step of commutation and depends on rotor angle. When the motor operates at low speed, adverse effects of this ripple could hinder smooth rotation of the rotor because filtering due to mechanical inertia is small [6]. It is possible to reduce the ripple, but this requires dedicated electronic hardware, which could be expensive to get or time-consuming to implement. Commutation and magnetic cogging produce periodic disturbance within the above DC motors. Accordingly, their effects on a motor shaft cannot be attenuated using mechanical gears. This usually makes it troublesome to employ the motors in high-precision trajectory control systems. However, such motors and the corresponding drives could be significantly more economical than AC alternatives.

A disturbance observer can be employed to estimate total disturbances due to loading torques applied at the motor shaft and modelling errors effectively [7-9]. This estimation requires knowledge of rotor angular acceleration. For trajectory control systems, the observer could take position feedback, and then use differentiators coupled with low-pass filters to estimate the acceleration. Preferably, the filters should be designed to have appropriate bandwidths so that satisfactory estimation of angular acceleration could be achieved. If the bandwidth of the filters is too high, undesirable noises could appear at the output, spoiling the estimation. Indeed, considering the fact that the acceleration signal is very active and noisy in general, designing such a filter could be challenging. To accommodate this, accurate velocity measurement could be a preferable solution to position measurement [10]. The quality of the signal can also be promoted by using high sampling frequency when the observer is implemented in a digital controller. Reducing modelling errors could attenuate the magnitude of disturbances and facilitate filter design, but this usually does not suppress noises significantly. When using a disturbance observer, the resulting estimation is always delayed by the use of low-pass filters, and thus produces estimation error. For practical cases in which the disturbances depend on time, the error is ultimately uniformly bounded by a positive number that depends on the time derivative of the disturbances [11]. Because of this, stability and performance of the resulting control system should be examined carefully [11, 12]. When a disturbance observer is used in DC motor motion control systems, classical linear control techniques relating to the concept of transfer function are usually adequate for stability and performance analysis. The analysis is generally conducted in the frequency domain because it allows effects of time delay to be shown clearly and conveniently.

When using a disturbance observer, one usually separates disturbance estimation from controller design of the associated nominal plant. The use of a disturbance observer allows independent investigation of the two components, although they both affect stability of the resulting control system [12]. In this paper, we make use of the above desirable characteristic. We propose an auxiliary linear control that can

be combined with existing linear controls in DC motor trajectory control systems to improve disturbance rejection.

Our controller design technique primarily differs from existing ones in two beneficial aspects. The first is that our development, which is all in state space, facilitates the use of existing results on robust stability to handle time-varying uncertainties in mass moment of inertia of the system. This feature greatly simplifies controller design and stability analysis. Secondly, our technique does not require feedback of electrical current in motor coils, which is mandatory for existing techniques. This reduces cost and complexity of the resulting control system. This also allows immediate use of our technique for improving disturbance rejection of existing trajectory control systems that do not have current feedback.

2. Mathematical Model

In this paper, we are interested in suppressing effects of rapidly fluctuating disturbance torque and parameter uncertainty on responses of existing DC-motor trajectory control systems. These include mechanically commutated brushed DC motors and electronically commutated 3-phase BLDC motors with trapezoidal back EMF. With commutation included, dynamical models of these electromechanical devices have the same structure [13-15]

$$J\ddot{\theta} + b\dot{\theta} = K_T i + T_d, \tag{2.1}$$

$$V - K_b\dot{\theta} = iR + L\left(\frac{di}{dt}\right), \tag{2.2}$$

where θ is the rotational angle of the motor rotor, i is the electrical current in the energized coils of the motor, V is the input voltage to the motor, and T_d is the disturbance torque applied to the rotor. Note that T_d represents both external loading torque and internal torque due to motor commutation and magnetic cogging. For brushed DC motors, torque ripple due to mechanical commutation could be insignificant when the number of rotor poles is large. For the above type of BLDC motors, we extensively employ a 6-step electronic commutation to energize two phases of the motor in certain sequences. This generally yields a large torque ripple as shown analytically in [4, 5], and also experimentally in [5]. This ripple is caused by phase switching, and its dynamic is very fast. It causes rough rotor rotation, which is clearly displayed when the angular speed is low. Handling this ripple involves electronic commutation design and is beyond our scope of discussion. All the physical parameters in the model are shown in Table 1. These must be determined specifically for the type of motor of interest. When the motor is coupled with mechanical transmission, the combined dynamic can be modeled by Eqs. (2.1)-(2.2) with a corresponding set of reflective parameters determined at output shaft of the transmission.

Table 1. Relevant parameters of DC motor.

Symbol	Meaning
J	mass moment of inertia (kg.m^2)
b	coefficient of viscous moment (N.m.s/rad)
K_T	torque constant (N.m/A)
K_b	speed constant (V.s/rad)
R	coil resistance (Ohm)
L	coil inductance (Henry)

In DC-motor motion control systems, parameters such as R, L, K_b, and K_T could be estimated or measured accurately using an appropriate group of basic measuring devices. However, this is not the case for the reflective mass moment of inertia J. This is partially because measuring J requires a specialized device. It could also be that the motor of interest is used to drive an object whose mass and shape can change

unpredictably with time, making J an uncertain time-varying function.

It can be shown that a state space description of the motor system in Eqs. (2.1)-(2.2) is

$$\begin{bmatrix} \dot{q}_1 \\ \dot{q}_2 \\ \dot{q}_3 \\ \dot{q}_4 \end{bmatrix} = \begin{bmatrix} 0 & 1 & 0 & 0 \\ 0 & 0 & 1 & 0 \\ 0 & 0 & -\frac{b}{J} & \frac{K_T}{J} \\ 0 & 0 & -\frac{K_b}{L} & -\frac{R}{L} \end{bmatrix} \begin{bmatrix} q_1 \\ q_2 \\ q_3 \\ q_4 \end{bmatrix} + \begin{bmatrix} 0 \\ 0 \\ 0 \\ \frac{1}{L} \end{bmatrix} V + \begin{bmatrix} 0 \\ 0 \\ \frac{1}{J} \\ 0 \end{bmatrix} T_d, \tag{2.3}$$

where $q_1 \equiv \int \theta \, dt$, $q_2 \equiv \theta$, $q_3 \equiv \dot{\theta}$, and $q_4 \equiv i$. Note that q_1 is included to allow applications of integration when designing controllers. The relevant dynamical variables that can be measured for feedback control are θ, $\dot{\theta}$, and i. The variable i can vary very quickly when compared to θ, and $\dot{\theta}$. Accurate reconstruction of $i(t)$ then requires correspondingly fast hardware, which could be inconvenient to acquire. Because existing control systems may not be equipped with such hardware, we want to avoid measuring i for feedback to broaden our scope of applications without significant loss of performance. For this, we recall that motor torque is proportional to i. To build torque quickly, servo motors are generally designed such that L is very small when compared to R and K_b. As an example, a Maxxon DC motor model RE65 with part number 353297 has nominal parameters $L = 0.161\times10^{-3}$ H, $R = 0.365$ Ohm, and $K_b = 8.15$ V.s/rad [16]. Because of this, it is reasonable to reduce Eq. (2.2) to:

$$V - K_b\dot{\theta} = iR. \tag{2.4}$$

We obtain from the above equation that $i = (-K_b\dot{\theta} + V)/R$ and substitute this in Eq. (2.1) to produce

$$\ddot{\theta} = -\left(\frac{K_T K_b}{JR} + \frac{b}{J}\right)\dot{\theta} + \left(\frac{K_T}{JR}\right)V + \left(\frac{1}{J}\right)T_d \ . \tag{2.5}$$

Recalling the three state variables $q_1 = \int \theta \, dt$, $q_2 = \theta$, $q_3 = \dot{\theta}$, we now model the dynamic of the motor using the reduced-order model

$$\dot{q} = Aq + Bu + NT_d, \tag{2.6}$$

where $q \equiv \begin{bmatrix} q_1 & q_2 & q_3 \end{bmatrix}^T$, $B \equiv \begin{bmatrix} 0 & 0 & b \end{bmatrix}^T$, $N \equiv \begin{bmatrix} 0 & 0 & n \end{bmatrix}^T$, $a \equiv -\left(K_T K_b / (JR) + b/J\right)$, $b \equiv K_T/(JR)$, $n \equiv 1/J$, $u \equiv V$, and $A = \begin{bmatrix} 0 & 1 & 0 \\ 0 & 0 & 1 \\ 0 & 0 & a \end{bmatrix}$. Notice that i is not a state variable in the above reduced-order model.

Our objective is to drive θ to track a given reference signal θ_r using an appropriate control input u. For this, a model representing the error dynamic of the control system is required. We now define three reference signals for the state variables q_1, q_2, and q_3 as $r_1 \equiv \int \theta_r \, dt, r_2 \equiv \theta_r$, and $r_3 \equiv \dot{\theta}_r$ respectively. The corresponding reference vector is $r \equiv \begin{bmatrix} r_1 & r_2 & r_3 \end{bmatrix}^T$. Now, let $e = r - q$, and substitute $q = r - e$, and $\dot{q} = \dot{r} - \dot{e}$ in the above equation to obtain the reduced-order error dynamics

$$\dot{e} = Ae + \bar{B}u + \bar{r} + \bar{N}T_d, \tag{2.7}$$

where $e = \begin{bmatrix} e_1 & e_2 & e_3 \end{bmatrix}^T$, $\bar{B} \equiv -B, \bar{N} \equiv -N$ and $\bar{r} \equiv -Ar + \dot{r} = \begin{bmatrix} \bar{r}_1 & \bar{r}_2 & \bar{r}_3 \end{bmatrix}^T$. When using the above error dynamical model for controller design, we do not need to measure i for feedback. Only relatively slow signals q_1, q_2, and q_3 are needed, allowing

applications of relatively slow measuring hardware.

In many situations, parameters in A and B are uncertain constants. However, they could also be uncertain time-varying functions in some situations. To accommodate these, we let $A = A_n + A_\Delta$ and $\bar{B} = \bar{B}_n + \bar{B}_\Delta$, where n and Δ denotes nominal and uncertain matrices respectively. Notice that the relevant matrices have the structures

$$A_n = \begin{bmatrix} 0 & 1 & 0 \\ 0 & 0 & 1 \\ 0 & 0 & a_n \end{bmatrix}, \quad A_\Delta = \begin{bmatrix} 0 & 0 & 0 \\ 0 & 0 & 0 \\ 0 & 0 & a_\Delta \end{bmatrix},$$

$$\bar{B} = \begin{bmatrix} 0 & 0 & \bar{b} \end{bmatrix}^T, \quad \bar{B}_n = \begin{bmatrix} 0 & 0 & \bar{b}_n \end{bmatrix}^T,$$

$$\bar{B}_\Delta = \begin{bmatrix} 0 & 0 & \bar{b}_\Delta \end{bmatrix}^T, \quad \bar{N} = \begin{bmatrix} 0 & 0 & \bar{n} \end{bmatrix}^T$$

The parameters a_n, and $\bar{b}_n$ are nominal values of $A(3, 3)$, and $\bar{B}(3, 1)$ respectively. In order to address the above general situations, the combined parameters a_Δ, and $\bar{b}_\Delta$ are allowed to be uncertain time-varying. It is reasonable to impose that we know nominal values, upper bounds, and lower bounds of all the parameters. This is equivalent to knowing $a_n, \bar{b}_n$, as well as upper bounds and lower bounds on a_Δ, and $\bar{b}_\Delta$. When all the uncertain matrices are zero, the resulting model is said to be nominal.

3. Controller Design

Consider applying the following two-part control law:

$$u = u_n + u_d, \tag{3.1}$$

where $u_n = -K_r e$ is the nominal control with $K_r = \begin{bmatrix} k_1 & k_2 & k_3 \end{bmatrix} \in \Re^3$, and u_d is the auxiliary control law that is intended to handle the disturbances and uncertainty. With the above control law, the error dynamical model now becomes

$$\dot{e} = (A + BK_r)e + \bar{B}u_d + \bar{r} + \bar{N}T_d.$$

To display uncertainty, the above equation can be written as

$$\begin{aligned} \dot{e} = {} & (A_n + B_n K_r)e + (A_\Delta + B_\Delta K_r)e \\ & + \bar{B}u_d + \bar{r} + \bar{N}T_d, \end{aligned} \tag{3.2}$$

where the gain matrix K_r is to be determined such that $A_n + B_n K_r$ is strictly stable. This can be achieved by applying an existing linear controller design technique to the nominal model $\dot{e} = A_n e + \bar{B}_n u_n$. The third state equation in Eq. (3.2) can be arranged as

$$\dot{e}_3 - \phi_{3n} = \bar{b}u_d + \phi_{3\Delta} + \bar{r}_3 + \bar{n}T_d,$$

In which $\phi_{3n} = a_n e_3 + b_n K_r e$, and $\phi_{3\Delta} = a_\Delta e_3 + b_\Delta K_r e$. By definition of $\bar{b}$, we know that $\bar{b} < 0$ and thus we should have that $\bar{b}_n < 0$. We define the nominal dynamic term β and the total disturbance term T_Σ as

$$\beta \equiv \dot{e}_3 - \phi_{3n}, T_\Sigma \equiv \phi_{3\Delta} + \bar{r}_3 + \bar{n}T_d,$$

where we note that T_Σ represents model uncertainty, and disturbance torque. It is desirable that $\beta = 0$ at all time because this implies nominal error dynamics for the system, in which the state vector e converges asymptotically to the origin by a selected stabilizing choice of K_r. If T_Σ is known, then it is simple to achieve this by using u_d. In practice, we cannot measure T_Σ directly because the parameters a_Δ and b_Δ are uncertain and T_d is unknown.

However, notice that $T_\Sigma = \beta$ when $u_d = 0$, and it is technically possible to estimate β. This allows us to estimate T_Σ indirectly, and then try to force that $\beta = 0$ by using u_d. This concept is central to the disturbance observer pioneered by Ohnishi [17] for speed control of DC motors. It has been applied and extended in many researches with good results [9]. A distinct advantage of this approach is that it separates controller design of the nominal system from total disturbance rejection. In particular, it can compensate quickly for sudden changes in loading torque when accurate angular acceleration of the rotor is available. This paper utilizes the above concept of disturbance observer to improve total disturbance rejection of existing DC motor trajectory control systems. Our approach differs from existing ones in that our development is all in state space, and *i* is not required for feedback. In addition, all parameters are allowed to be time-varying, and a sufficient condition for input-to-state stability of the resulting control system is clearly stated. In this paper, we propose to reduce the magnitude of β by using the auxiliary control input:

$$u_d = -\frac{\gamma}{b_n}(\dot{e}_{3f} - \phi_{3n}), \tag{3.3}$$

in which $\dot{e}_{3f} = \ddot{\theta}_r - \ddot{\theta}_f$, $\ddot{\theta}_f$ is the output of a Low-Pass Differentiator (LPD) whose input is the measured angular velocity $q_3 = \dot{\theta}$ of the rotor, and $1 \geq \gamma > 0$ is a design parameter. A large value for γ represents strong effort of compensation for total disturbance. When the bandwidth of LPD is very high, this could cause state oscillation. Our investigation reveals that a simple LPD could yield satisfactory results with $0.9 \geq \gamma \geq 0.5$.

Because of the previously imposed structure of u_n, the resultant control law $u = u_n + u_d$ is a linear state-feedback law in which four feedback signals, namely $\int \theta\, dt$, $\theta, \dot{\theta}$, and $\ddot{\theta}_f$, are used. Out of these four, we need to measure only θ, and $\dot{\theta}$ because the other two can be readily obtained from them. This control can be written in vector-matrix form as shown:

$$\begin{aligned} u &= -K_r e + \frac{\gamma}{b_n}\dot{e}_{3f} - \gamma\frac{a_n}{b_n}e_3 - \gamma K_r e, \\ &\equiv -K_{rf} e_{rf}, \end{aligned} \tag{3.4}$$

in which $K_{rf} = \left[c_1 k_1 \;\middle|\; c_1 k_2 \;\middle|\; c_1 k_3 - c_2 \;\middle|\; c_3\right]$, $c_1 \equiv (1+\gamma), c_2 = \gamma(a_n / b_n), c_3 = -\gamma / b_n$, and $e_{rf} \equiv \left[e_1 \;\; e_2 \;\; e_3 \;\; \dot{e}_{3f}\right]^T$. Our control input u is obtained from θ and $\dot{\theta}$, without using *i*, as desired. However, using $\ddot{\theta}_f$ to implement the control input actually introduces additional dynamic to the feedback loop. This dynamic will be augmented to the full-order model in Eq. (2.3) such that the resulting model could be useful for examining stability of the resulting control system.

Our LPD is a differentiator cascaded with a low-pass filter. The input of the LPD is the angular velocity $q_3 = \dot{\theta}$, and the output is $\ddot{\theta}_f \equiv q_5$. For simplicity, we use a first-order low-pass filter and propose the following transfer function for this LPD:

$$\frac{Q_5(s)}{Q_3(s)} = \frac{a_{fa} s}{s + a_{fa}}, \tag{3.5}$$

where $a_{fa} \in \Re^+$ is a design parameter, $Q_3(s)$ is the Laplace transform of filter input q_3, and $Q_5(s)$ is the Laplace transform of filter output q_5. The parameter a_{fa} simultaneously affects bandwidth and gain of the LPD, performance of disturbance rejection, and stability of the

resulting control system. Primarily, the parameter should be chosen so that the bandwidth of the LPD contains frequency of the disturbance torque to be rejected. Noting that the above transfer function is not strictly proper, it is straightforward to show that a state-space representation of the LPD is:

$$\dot{w}_1 = -a_{fa} w_1 + q_3,$$
$$q_5 = -a_{fa}^2 w_1 + a_{fa} q_3,$$

where w_1 is the only state variable of the LPD. Dynamics of the LPD can be augmented to the full-order model in Eq. (2.3) to produce the following expanded model:

$$\dot{q}_f = A_f q_f + B_f u + N_f T_d \ , \qquad (3.6)$$

where

$$q_f \equiv \left[q_1 \,\middle|\, q_2 \,\middle|\, q_3 \,\middle|\, q_4 \,\middle|\, w_1 \right],$$
$$B_f \left[0 \;\; 0 \;\; 0 \;\; (1/L) \;\; 0 \right]^T,$$
$$N_f \left[0 \;\; 0 \;\; (1/J) \;\; 0 \;\; 0 \right]^T,$$
$$A_f = \left[\begin{array}{cccc|c} 0 & 1 & 0 & 0 & 0 \\ 0 & 0 & 1 & 0 & 0 \\ 0 & 0 & -\frac{b}{J} & \frac{K_T}{J} & 0 \\ 0 & 0 & -\frac{K_b}{L} & -\frac{R}{L} & 0 \\ \hline 0 & 0 & 1 & 0 & -a_{fa} \end{array}\right].$$

We now rewrite the control law u to accommodate the increased dimension of the system. Let us denote the *i*-th element of K_{rf} by k_{rfi}, i = 1, 2,…, 4. With this, it can be shown that $u \equiv -K_{rf} e_{rf}$ can be written as

$$u = K_f q_f - K_g r_g \ , \qquad (3.7)$$

where

$$K_f \equiv \left[k_{rf1} \,\middle|\, k_{rf2} \,\middle|\, k_{rf3} + k_{rf4} a_{fa} \,\middle|\, 0 \,\middle|\, -k_{rf4} a_{fa}^2 \right],$$
$$K_g \equiv \left[k_{rf1} \,\middle|\, k_{rf2} \,\middle|\, k_{rf3} \,\middle|\, 0 \,\middle|\, k_{rf4} \right], \text{and}$$
$$r_g \equiv \left[r_1 \,\middle|\, r_2 \,\middle|\, r_3 \,\middle|\, 0 \,\middle|\, \ddot{\theta}_r \right]^T.$$

By defining $r_f \equiv \left[r_1 \,\middle|\, r_2 \,\middle|\, r_3 \,\middle|\, 0 \,\middle|\, 0 \right]^T$ and $e_f \equiv r_f - q_f$, error dynamic of the expanded system can be written as

$$\dot{e}_f = \tilde{A}_f e_f + p(t), \qquad (3.8)$$

where $\tilde{A}_f \equiv A_f + B_f K_f$, $p(t) \equiv \bar{r}_f + \bar{N} T_d$, and $\bar{r}_f \equiv -\tilde{A} r_f + \dot{r}_f + B_f K_g r_g$. Now, let $A_f \equiv A_{fn} + A_{f\Delta}$ and $B_f \equiv B_{fn} + B_{f\Delta}$, where n and Δ denote nominal values and uncertain time-varying functions respectively. Using these, the above error dynamical model can be written as

$$\dot{e}_f = (A_{fn} + B_{fn} K_f) e_f + (A_{f\Delta} + B_{f\Delta} K_f) e_f + p(t).$$

This allows us to write the model in a form that is suitable for examining stability:

$$\dot{e}_f = \tilde{A}_{fn} e_f + \textstyle\sum_{j=1}^{N} [h_j(t) E_j] e_f + p(t), \qquad (3.9)$$

where $\tilde{A}_{fn} \equiv A_{fn} + B_{fn} K_f$, $E_j \in \Re^{n \times n}$ is known, and $h_j(t) \in \Re$ is an uncertain time-varying function with known upper bound $h_{uj} \geq h_j$ and lower bound $h_{lj} \leq h_j$.

In simple cases in which all parameters in $A_{f\Delta}$ and $B_{f\Delta}$ are uncertain constants, $h_j(t)$ is constant for all *j*. Then, we need only to choose K_r, γ, and a_{fa} such that the resulting K_f strictly stabilizes $\tilde{A}_f$ for all possible parameters. This is usually straightforward to achieve. However, there are some cases in which stability of $\tilde{A}_f$ does not imply stability of

the control system. These include cases in which mass or shape of an object driven by the motor changes rapidly, making the reflective mass moment of inertia J an uncertain time-varying function. To handle all these cases simultaneously, we view $p(t)$ as a bounded perturbation vector entering the time-varying system $\dot{e}_f = \tilde{A}_f e_f$. Then we apply an existing robust stability theorem to determine if the origin of the system is uniformly globally exponentially stable when $p(t) = 0$. When this type of stability is confirmed, it can be shown that the origin of the perturbed system is input-to-state stable [18], guaranteeing that all trajectories converge to a neighborhood about the origin. The extent of this neighborhood depends on the magnitude of p(t), which is a reasonable outcome. We provide the following robust stability theorem and a corollary for convenience of the readers.

Theorem 1. If a dynamical system can be represented by Eq. (3.9) with $p(t) = 0$, and the right-hand side of the equation is uniformly globally Lipschitz with $\tilde{A}_{fn}$ being Hurwitz, then the equilibrium point at the origin is uniformly globally exponentially stable when all the real eigenvalues of the matrix $Z = Z^T \in \Re^{n\times n}$ are negative. The matrix Z is obtained by

1) Specified $Q > 0$ to compute P from the Lyapunov equation:
$-Q = (1/2)[P\tilde{A}_{fn} + \tilde{A}_{fn}^T P],$
2) Compute $\tilde{A}_l = \tilde{A}_{fn} + \sum_{j=1}^{N} h_{lj} E_j,$ and $\Phi = P\tilde{A}_l + \tilde{A}_l^T P.$
3) Compute $\Psi_j = [PE_j + E_j^T P] = \Psi_j^T, \forall j.$
4) Compute
$\Lambda_{\Psi_j} = T_{\Psi_j}^T \Psi_j T_{\Psi_j} = diag[\lambda_{\Psi_j 1} \ \dots \ \lambda_{\Psi_j n}],$
$\forall j$
Where
$T_{\Psi_j} = [v_{\Psi_j 1} \mid \dots \mid v_{\Psi_j n}],$
$\{v_{\Psi_j 1}, \dots, v_{\Psi_j n}\}$ is the set of n orthogonal unit (orthonormal) eigenvectors of Ψ_j, and $\{\lambda_{\Psi_j 1}, \dots, \lambda_{\Psi_j n}\}$ is the corresponding set of n real eigenvalues of Ψ_j.
5) Set all negative elements of Λ_{Ψ_j} to zero to get $\Lambda_{\Psi_j}^{\geq 0}, \forall j$.
6) Compute $\Psi_j^{\geq 0} = T_{\Psi_j} \Lambda_{\Psi_j}^{\geq 0} T_{\Psi_j}^T, \forall j$.
7) Compute $Z \equiv \Phi + \sum_{j=1}^{r} [(h_{uj} - h_{lj}) \Psi_j^{\geq 0}]$.

Proof. See [19].

Corollary 1. If Theorem 1 is satisfied, then trajectories of Eq. (3.9) with $p(t) \neq 0$ converge to a neighborhood about the origin. The extent of this neighborhood is defined by

$$\Omega = \{x \mid V(x) \leq (1/2)\max(\lambda_P)\sigma^2\},$$

where $V(x) = (1/2)x^T Px$, $P = P^T > 0$ is obtained from Theorem 1, λ_P is the set of all eigenvalues of the matrix P, $\sigma = 2\phi \max(\lambda_P) / |\max(\lambda_Z)|$, and ϕ is a bound on $p(t)$.

Proof. See [20].

To summarize our development, we begin by considering a DC-motor trajectory control system that is stabilized by its nominal control u_n when all of its relevant parameters are at their nominal values. We want to enhance its disturbance rejection by augmenting an auxiliary control u_d, which also guarantees its stability when some parameters become time-varying. The nominal linear state feedback gain matrix K_r should be made available first. Then, the auxiliary control requires that we choose two design parameters, namely γ and a $_{fa}$. Both affect strength and speed of

disturbance rejection simultaneously. Combining the two control components, we obtain the resultant control input $u \equiv -K_{rf} e_{rf}$ and the gain matrix K_f. Using K_f and uncertainty specifications associated with $A_{f\Delta}$ and $B_{f\Delta}$, we employ Theorem 1 to determine if the resultant control input guarantees input-to-state stability of the control system. According to this development, our controller design procedure is shown in the next section.

4. Examples

In our control system, a brushed DC motor is coupled with a multi-stage mechanical transmission system, whose output shaft is used to rotate an object along prescribed trajectories. Our measurement indicates that $R = 6\ \Omega$, and $L = 1.3\times10^{-3}\ H$. With q_2 being the rotational angle of the output shaft in radians, we have verified that reflective values of the parameters at the output shaft are $K_T = 0.31$ N.m/A, $K_b = 0.9$ V.s/rad, and $b = 2\times10^{-4}$ N.m.s/rad. Due to changes in mass and shape of the object mounted on the output shaft, the reflective mass moment of inertia is an uncertain time-varying function. It appears that the nominal value J(t) is $J_n = 3\times10^{-3}$ kg.m^2, and the variation of $J(t)$ is $J_n \le J(t) \le 1.25J_n$. The 25% uncertain time-varying increase of $J(t)$ from J_n translates to 20% of time-varying uncertainty in two elements of A_f, namely $A_f(3,3)$, and $A_f(3,4)$:

$$-\frac{b}{J_n} \le A_f(3,3) \le -\frac{b}{J_n} + 0.2\left(\frac{b}{J_n}\right),$$

$$\frac{K_T}{J_n} - 0.2\left(\frac{K_T}{J_n}\right) \le A_f(3,4) \le \frac{K_T}{J_n}.$$

Let the uncertain time-varying functions $h_1(t)$ and $h_2(t)$ correspond to $A_f(3,3)$, and $A_f(3,4)$. It follows that

$$h_1(t) \in \left[0,\ 0.2\left(\frac{b}{J_n}\right)\right],\ h_2(t) \in \left[-0.2\left(\frac{K_T}{J_n}\right),\ 0\right].$$

The associated matrices E_1 and E_2 belong to $\Re^{5\times5}$. All of their elements are zero except $E_1(3,3) = 1$, and $E_2(3,4) = 1$. The control system is subjected to loading torque $T_d = T_{d1} + T_{d2}$, in which T_{d1} is the cogging torque at the rotor, and T_{d2} is the loading torque at the output shaft. When the object is rotated along a normal trajectory, we approximate that $T_{d1} = \mathrm{a_{Td}}\ (\sin(48\theta) + 1)$ and $T_{d2} = 2\mathrm{a_{Td}}\sin(\omega_{Td}\mathrm{t})$, where $\mathrm{a_{Td}} = 0.25K_T$ and $\omega_{Td} = 0.4$ rad/s. Note that T_{d1} and T_{d2} depend on rotor angle and time, respectively, and that the magnitude of cogging torque is as high as 25% of K_T. Using the above data, our controller design procedure can be conducted as shown in the following.

Without i as a feedback signal, our nominal control is obtained by using the reduced-order error dynamic modeled by Eq. (2.7) with $u = u_n = -K_r e$. For this, note that the values of R, K_T, K_b, and b are given previously, while J is set to J_n, not considering uncertainty at this point. The well-known LQR is employed to minimize the cost function

$$J_c = \int_0^\infty (e^T Q e\ +\ u_n^T R u_n) dt,$$

where $Q = 0.05I_{3\times3}$, and R = [1]. This yields

$$K_r = \begin{bmatrix} -0.22 & -0.7 & -0.07 \end{bmatrix}.$$

The above gain matrix locates the eigenvalues of $A_n + B_n K_r$ at $s = -16.03$, and $\mathrm{s} = -0.37 \pm 0.33i$, implying that that reduced-order model is strictly stable. Next,

with availability of K_r and the nominal values a_n and b_n defined previously, selecting $\gamma = 0.75$ yields the resultant control input $u = -K_{rf} e_{rf}$ in which

$$K_{rf} = \begin{bmatrix} -0.39 & -1.22 & -0.8 & -0.04 \end{bmatrix},$$

and we select the LPD parameter $a_{fa} = 10$ to obtain the last element of e_{rf}. The value of this parameter is chosen so that the LPD bandwidth contains frequency of the cogging torque when the magnitude of $\dot{\theta}$ is greater than 0.2 rad/s.

Now that the resultant control input is already obtained, we examine stability of the resulting control system. For this, we write the resultant control input as $u = K_f q_f - K_g r_g$ in which

$$\mathrm{K}_f = \left[\begin{array}{c|c|c|c|c} -0.39 & -1.22 & -1.24 & 0 & 4.35 \end{array}\right],$$

$$K_g = \left[\begin{array}{c|c|c|c|c} -0.39 & -1.22 & -0.8 & 0 & -0.04 \end{array}\right].$$

The above form of resultant control leads to the full-order model of error dynamic shown in Eq. (3.9). The five eigenvalues of $\tilde{A}_{fn} \equiv A_{fn} + B_{fn} K_f$ are $s = -0.36 \pm j0.32$ $s = -385.43 \pm j149.71$, and $s = -7.72$, implying that the full-order nominal model is strictly stable. It now remains to show that the control system is stable in presence of the uncertain time varying mass moment of inertia $J(t)$. Given the above upper and lower bounds on $h_1(t)$ and $h_2(t), E_1$, and E_2, it can be shown that the maximum eigenvalue of Z in Theorem 1 is $\max(\lambda_Z) = -13.5 < 0$. Accordingly, the resulting control system is input-to-state stable by Theorem 1. This corresponds to the following symmetric matrices.

$$Q = \left[\begin{array}{c|c|c|c|c} 9.5 & 0 & 0 & 0 & 0 \\ \hline . & 20 & 0 & 0 & 0 \\ \hline . & . & 19 & 0 & 0 \\ \hline . & . & . & 19 & 0 \\ \hline . & . & . & . & 21 \end{array}\right],$$

$$Z = \left[\begin{array}{c|c|c|c|c} -18 & 2.29 & 1.51 & -3.18 & -1.41 \\ \hline . & -34.4 & 3.7 & -7.82 & -3.46 \\ \hline . & . & -35.5 & -5.15 & -2.28 \\ \hline . & . & . & -27.1 & 4.82 \\ \hline . & . & . & . & -39.8 \end{array}\right].$$

We now employ numerical simulations to investigate performance of the control system using the full-order model in Eq. (3.6). For this, the reference trajectory of the output shaft is $\theta_r(t) = 10\sin(0.15t)$, and the reflective mass moment of inertia is approximated by

$$J(t) = J_n + 0.125 J_n(\sin(2\omega_r t) + 1),$$

where $\omega_r = 0.15$ rad/s. This exact expression of $J(t)$ is not required for our controller design procedure. In all simulations, the initial condition is set to $q_f(0) = \left[\begin{array}{c|c|c|c|c} 0 & 5 & 0 & 0 & 0 \end{array}\right]^T$. The simulation results in Figs. 1-2 are trajectories of output shaft rotational angle $\theta(t)$ for the cases in which the auxiliary control is absent and present. Figs. 3-4 show trajectories of output shaft angular velocity $\dot{\theta}(t)$, Fig. 5 shows the disturbance torque $T_d(t)$, and Figs. 6-7 show the control input $u(t)$ for both cases. It appears in Figs. 1-2 that the two trajectories converge to the reference trajectory $\theta_r(t)$. Tracking error in the case with auxiliary control is approximately 40% less than that in the case without auxiliary control for most of the time. Figs. 3-4 display clearly a very undesirable effect of the cogging torque, which causes oscillation of the angular velocity about its reference trajectory. However, the auxiliary control can suppress the magnitude of oscillation by approximately 40% for most of the time. As the frequency of oscillation increases, the suppression gets better. We can see from Fig. 5 that the magnitudes of disturbance torque T_d in both cases are approximately

the same during the course of simulation. Notice that the torque comprises cogging torque with high frequency and low magnitude and loading torque with low frequency and high magnitude.

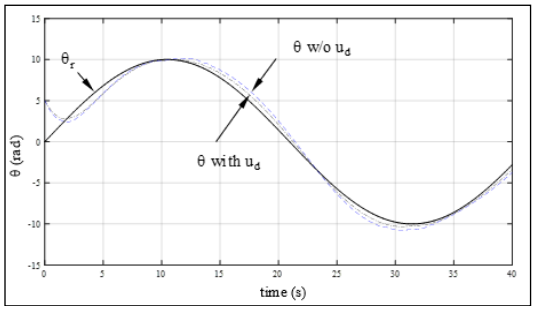

Fig. 1. Reference trajectory θ_r (-), Simulated Trajectory θ with u_d (.-), and without u_d (--).

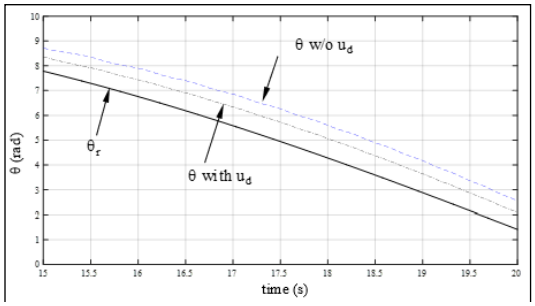

Fig. 2. Reference trajectory θ_r (-), Simulated Trajectory θ with u_d (.-), and without u_d (--).

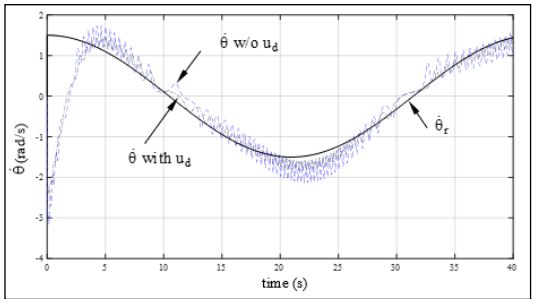

Fig. 3. Reference trajectory $\dot{\theta}_r$ (-), Simulated Trajectory $\dot{\theta}$ with u_d (.-), and without u_d (--).

The resultant control inputs with and without the auxiliary control are shown in Figs. 6-7. We see from these figures that the magnitudes of the two signals are about the same, except that the control input with auxiliary control reacts to the disturbance torque much faster than the other control input does. This characteristic is very beneficial for handling high-frequency disturbance torque that constantly occurs. It then appears that the auxiliary control can reduce both tracking error and output oscillation by its superior responding speed. It does so without using a large magnitude of control input, which is desirable when considering cost of implementation. It appears in our investigation that the tracking error could be made smaller than that shown in Figs. 1-2 by using a stronger nominal control or a larger γ. However, we do not pursue this because the present result is already sufficient to display the benefit of our auxiliary control.

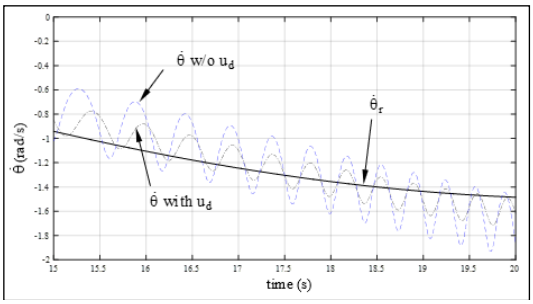

Fig. 4. Reference trajectory $\dot{\theta}_r$ (-), Simulated Trajectory $\dot{\theta}$ with u_d (.-), and without u_d (--).

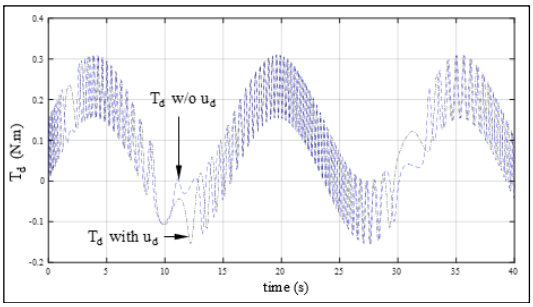

Fig. 5. Disturbance Torque T_d with u_d (.-), and without u_d (--).

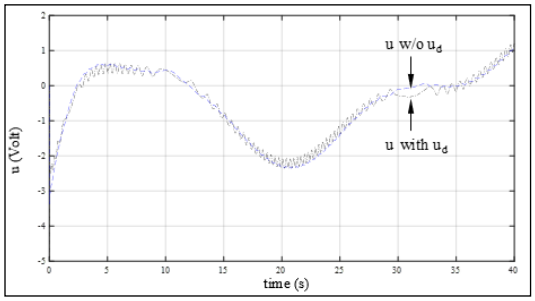

Fig. 6. Control with u_d (.-), and without u_d (--).

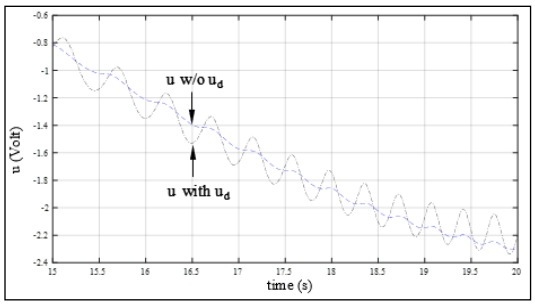

Fig. 7. Control with u_d (.-), and without u_d (--).

5. Conclusion

DC motors are usually used as driving actuators in trajectory control systems where a large magnitude of torque is required at economical cost. In some situations, the systems are supposed to handle external loading torque and uncertain time-varying mass moment of inertia associated with their operations. When implementation cost is of great concern, the control systems are to handle cogging torque normally found in economical DC motors. These torques are primary causes of tracking errors and output oscillation, and it is particularly important that the control systems can reject these undesirable effects efficaciously. Also, they must be robustly stable when subjected to time-varying uncertainty of reflective mass moment of inertia in some situations.

Our strategy for rejecting tracking error and output oscillation due to disturbance torques is to augment an auxiliary linear control to existing linear robust controls. Our auxiliary control is motivated by the known concept of disturbance observer. When the concept is applied to motion control of DC motors, it usually appears that coil current is used as a feedback signal and transfer function is the analytical tool of choice. However, our implementation does not require coil current as a feedback signal. Our development is all conducted in state space and allows writing error dynamic of the control system in a form that facilitates assertion of stability. It is the essence of the auxiliary control that an estimation of angular acceleration is required in order to response quickly to disturbances. This signal is obtained as the output of a low-pass differentiator whose input is the available angular velocity. In here, the differentiator is cascaded with a first-order low-pass filter for simplicity. Stability of the resulting control system can be theoretically confirmed by using an existing robust stability theorem.

We investigate performance of the control systems with and without the auxiliary control by means of numerical simulations. It appears that the output of the control system with our auxiliary control converges to the reference trajectory as indicated by the provided robust stability theorem. The auxiliary control affects speed of convergence only slightly. However, it can reduce satisfactorily the magnitude of tracking error and oscillation of the output due to disturbance torque as formulated. It primarily accomplishes these by reacting swiftly, not by increasing the magnitude of the control signal. This desirable characteristic allows its uses in existing control systems without need to increase capacity of the associated amplifiers.

References

[1] Padmaraja Y. Hands-on Workshop: Motor Control Part 4 -Brushless DC (BLDC) Motor Fundamentals. Microchip AN885; 2003.

[2] Hakan G. Industrial Motion Control: Motor Selection, Drives, Controller

Tuning, Application. John Wiley & Sons; 2016.

[3] Ramu K. Permanent Magnet Synchronous and Brushless DC Motor Drives. Taylor and Francis; 2010.

[4] Renato C. et. al. Analysis of torque ripple due to phase commutation in brushless DC machines. IEEE Trans. Ind. Appl. 1992;28: 632-8.

[5] Xinmin Li et. al. Commutation torque ripple suppression strategy of brushless DC motor considering back electromotive force variation. Energies. 2019;12:21.

[6] Austin H. Electric motors and drives: fundamentals, types and applications: third edition. Elsevier; 2006.

[7] Kouhei O., Masaaki S., Toshiyuki M. Motion control for advanced mechatronics. IEEE/ASME Trans. Mechatronics. 1996;1:1: 56-67.

[8] Ho SL., Masayoshi T. Robust motion controller design for high-accuracy positioning systems. IEEE Trans. Ind. Electron. 1996;43:1: 48-55.

[9] Emre S., Roberto O., Kouhei O. "Disturbance Observer-based robust control and its applications: 35th anniversary overview," IEEE Trans Ind Electron 2020;67:3: 2042-53.

[10] Tsuji T., Hashimoto T., Kobayashi H., Mizuochi M., Ohnishi K. A wide-range velocity measurement method for motion control. IEEE Transactions on Industrial Electronics. 2009;56:2: 510-9.

[11] Emre S., Kouhei O. A guide to design disturbance observer. ASME Trans. J. Dyn. Sys. Meas. Control 2014;136:2: 1-10.

[12] Emre S., Kouhei O. Stability and robustness of disturbance observer based motion control systems. IEEE Trans Ind Electron. 2015;62:1: 414-22.

[13] Timothy JEM. Brushless permanent-magnet and reluctance motor drives. Oxford University Press; 1989.

[14] Chang LX. Permanent magnet brushless DC motor drives and controls. Singapore: John Wiley & Sons; 2012.

[15] Ali E. Advanced Electric Drive Vehicles. CRC Press; 2015.

[16] Maxon Motor AG. Selection guide: program 2017/2018. Switzerland; 2017.

[17] Kiyoshi O., Kouhei O., Kullio M. Torque – speed regulation of DC motor based on load torque estimation method. International Power Electronics Conference. 1983; 1209-18.

[18] Hassan KK. Nonlinear systems, 3rd edition. NJ: Prentice Hall; 2000.

[19] Pinit N. A graphical robust PID controller design for time-varying uncertain systems with applications to trajectory tracking of a load-varying rigid SCARA. Thammasat International Journal of Science and Technology. 2016;21:2: 34-44

[20] Pinit N. Using adaptive integral gain for overshoot reduction in PID control systems. Sciences & Technology Asia. 2019;24:2: 34-44.